Effect of the deposition conditions on the anion resin exchange precipitation of indium (III) hydroxide

Journal:	*ACS Omega*
Manuscript ID	ao-2019-03877g
Manuscript Type:	Article
Date Submitted by the Author:	14-Nov-2019
Complete List of Authors:	Evsevskaya, Natalia; Institut himii i himiceskoj tehnologii SO RAN, Pikurova, Elena; Institut himii i himiceskoj tehnologii SO RAN Saikova, Svetlana; Krasnoyarsk State University of Non-Ferrous Metals and Gold Nemtsev, Ivan; Krasnoarskij naucnyj centr SO RAN

Effect of the deposition conditions on the anion resin exchange precipitation of indium (III) hydroxide

Natalia Evsevskaya[a*], Elena Pikurova[a], Svetlana Saikova[a,b], Ivan Nemtsev[c,d]

[a]*Institute of Chemistry and Chemical Technology SB RAS, Federal Research Center "Krasnoyarsk Science Center SB RAS", Akademgorodok 50,bld. 24, Krasnoyarsk, 660036, Russia;*

[b]*Siberian Federal University, Svobodny st, 79, Krasnoyarsk, 660041, Russia;*

[c]*Federal Research Center "Krasnoyarsk Science Center SB RAS" Akademgorodok 50, Krasnoyarsk, 660036, Russia;*

[d]*Kirensky Institute of Physics, Federal Research Center "Krasnoyarsk Science Center SB RAS", Akademgorodok 50,bld. 38, Krasnoyarsk, 660036, Russia.*

Abstract

A new patented method for the synthesis of nanosized powders of indium (III) hydroxide and oxide using the strong base anion exchange resin AV-17-8 as a precipitate agent was proposed. The effect of anions of the initial indium salt as well as the influence of the process duration, temperature, and counterions of resin such as hydroxide or carbonate on the yield of indium (III) hydroxide during the anion resin exchange precipitation was investigated by SEM, electrical conductivity measurement method and atomic absorption analysis. Based on the obtained data, the mechanism of the anion resin exchange precipitation of indium (III) hydroxide was suggested. The products were characterized by XRD,

TGA/DSC, elemental analysis, BET, and TEM. It was found that impurity-free monophasic In_2O_3 powders with the average particle size of 10-15 nm and specific surface area of 62-73 m^2/g were formed after heat treatment of as-prepared products at 400 °C.

Key words: Indium oxide, indium hydroxide, nanoparticles, anion resin exchange synthesis

Introduction

Indium (III) oxide, In_2O_3, is an optically transparent (in the visible range (80-90%)) semiconductor oxide with high electrical conductivity. Thus, In_2O_3 is widely used for the production of numerous optical-electronic devices equipped with touch screens, LCD and plasma TVs, solar cells and highly sensitive gas sensors.[1-5] In electronics one of the most popular materials is indium tin oxide (ITO), representing a mixture of In_2O_3 and SnO_2, usually in a mass ratio of 9: 1.[6,7]

Generally, the materials based on indium oxide are obtained from the high reactive precursor $In(OH)_3$ because its characteristics directly affect the properties of the product. Therefore, the development of new synthetic strategies for the production of indium (III) hydroxide with chemical homogeneity, containing particles of similar size and morphology, is a current problem.

The most common methods used to synthesize $In(OH)_3$ are the chemical precipitation from salt solution,[8-12] hydrothermal or solvothermal synthesis,[13-18] sol – gel process[19,20] and their combinations[21,22]. In the case of the solvothermal (hydrothermal) process the initial salts of indium or as-precipitated $In(OH)_3$ are kept in an autoclave in aqueous solution or organic solvents at high temperature and pressure, usually, in the presence of surfactants. This approach allows one to obtain products with precisely defined morphology (nanorods, nanocubes, hollow spheres, etc.), and the finest products as compared with other methods. However, the solvothermal method requires the use of complex, expensive equipment, high pressure, being limited by the small size of the reaction chambers. For the sol-gel synthesis, expensive gel-forming components are used, and long synthesis time is required, as well as the control of the hydrolysis rate of the initial reagents in order to avoid micro-heterogeneity in the system.

The chemical precipitation method requires the control of the pH value and reaction conditions. Also, as-prepared precipitate particles tend to trap the mother liquor ions; therefore, long-term thorough washing is needed to remove all the adsorbed species, which results in the formation of a large amount of rinsing water subject to disposal. Each technique presented has some disadvantages, therefore, the creation of new modifications of the known method is an urgent problem.

For the synthesis of precursors of oxide materials the so-called anion resin exchange precipitation of metal ions is perspective.[23-26] Ion-exchange resins are widely used in different separation, purification, and decontamination processes. In the case of anion resin exchange precipitation, a resin or polymer acts as a reagent.

This method involves two combined heterogeneous reactions: anion exchange between the sorbent solution and precipitation of an insoluble metal compound from the solution. The process of obtaining $In(OH)_3$ can be described by the equations:

$$InA_3 + 3ROH = In(OH)_3\downarrow + 3RA, \quad (1)$$

$$2InA_3 + 3R_2CO_3 + (3-2x)H_2O = 2In(OH)_{3-2x}(CO_3)_x\downarrow + 6RA + (3-2x)CO_2\uparrow, \quad (2)$$

R is the anion-exchange resin, ($A = Cl^-$, $1/2SO_4^{2-}$, NO_3^-).

This process should be considered as a special case of ion exchange complicated by the precipitation reaction. The method results in nearly complete conversion of reagents and high selectivity, reducing material and energy costs associated with eliminating the necessity of additional purification of products, and, as a result, simplifying the technology design of production, as reported in.[27]

Herein, we propose the anion resin exchange precipitation method of obtaining $In(OH)_3$ and In_2O_3 powders patented by us.[28] As far as we know, the anion resin exchange precipitation method was not used earlier to produce these materials. The influence of various conditions on this process was investigated and the obtained products were characterized.

Results and discussion

Anion resin exchange precipitation of indium (III) hydroxide

To control reactions 1 and 2, the specific electrical conductivity of the reaction solutions was measured during the synthesis (Figure 1). The chemical reaction of the anion resin exchange precipitation reduces the number of ions in the

solution because the anions of the initial indium salt are absorbed by the resin and the In^{3+} ions are bound into a solid product with ions from the resin: In-OH – for the OH-form and In-CO_3 for R-CO_3. Uncharged species in the solution do not carry any charge, then a decrease of the specific electrical conductivity of the reaction solution is observed. As we discussed earlier,[29] in the case of the anion resin exchange precipitation the charge and diameter of hydrated anions are the main factors affecting the effectiveness of the process. As can be seen in Fig 1, when $In_2(SO_4)_3$ is used, the SEC of the solution goes down to zero rapidly (30 min), and the formation of a dense white precipitate is observed. In the case of using other indium salts, $In(NO_3)_3$ or $InCl_3$, after 1 h the SEC reaches about 100 μS/m and remains constant over time. Moreover, the precipitate formation does not occur, but sols are formed, which are transformed into gels with time. In general, the extent of precipitation of indium ions decreases in the row $In_2(SO_4)_3$> $InCl_3$≈In $(NO_3)_3$, which is in agreement with the order of affinity for strongly basic anion exchangers.[27] In the subsequent experiments the anion resin exchange precipitation of indium was carried out only from its sulphate solutions.

It was found[30] that more reactive precursors with higher surface area are formed if to use the resin in the CO_3-form as compared to the OH-form due to carbon dioxide release during the process (reaction 2) and further heat treatment (Fig. 2).

Figure 1b shows the time-dependence of the specific electrical conductivity of the solutions during the anion resin exchange precipitation of indium (III) sulfate in the presence of the resins in OH- and CO_3-forms. The precipitation was

faster when the carbonate form of resin was used: the SEC of the solution was dramatically decreased to zero during 10 min. This can account for the fact that in this case a higher pH value of 7,5 versus 6 was gained when using the anion exchange resin in the hydroxide form. The results can also be confirmed by the distribution ratios of indium between the phases of the solution, the precipitate, and the resin during precipitation (Fig. 3). The concentration of In^{3+} in the solution was crucially decreased to 2 % of its initial concentration during 10 min after the start of the synthesis when the resin in the carbonate form was used (Fig. 3, curve 3b), whereas the precipitation in the presence of the resin in OH-form occurred within 25 min (Fig. 3, curve 3a). However, the indium hydroxide yield for this time was low (55 and 65 %, respectively), due to a significant amount of indium hydroxide (15 and 27 %) being deposited on the resin bead surface (Fig. 3, curves 2a and 2b). Then, during further precipitation the product yield (Fig. 3, curves 1a and 1b) increased up to 96 and 88 % during 24 h for OH- and CO_3-forms of the resin, respectively. At the same time, the amount of indium in the resin phase decreased.

According to electron microscopy (Figure 4), after 15 min of the synthesis the surface of the resin beads was almost completely covered by a layer of a surface deposit with the thickness of about 1.5 μm. These data are given for the carbonate form of resin, and the results obtained for OH-form are similar. According to energy-dispersive X-ray spectroscopy (Figure 5a and 5b), the composition of the surface deposit corresponds to the crystals deposited on the bottom. A small amount of sulfur (0.4 %) and carbon might be explained by the fact that the resin composition was determined through the layer of deposit or its

cracks, since sulfur in the product was not detected. The surface deposit started to flake away from the resin beads after 30-60 minutes since the areas of the cleared bead surfaces could be seen. The thickness of the remaining deposited layer was about 1 μm. The deposit is assumed to have been desorbed when reaching the thickness of more than 1.5 μm. The SEM data revealed that the complete desorption occurred within 24 h.

Thus, based on the data of chemical analysis and microscopy we can suggest the following mechanism of the anion resin exchange precipitation of indium (III) hydroxide. The first stage is the anion exchange between the anions of indium solution and the resin; then, the formation of indium hydroxide starts on the surface of the resin beads and finally after the thickness of the deposit layer increases to 1.5 μm and more, it flakes away from the resin beads and settles onto the vessel bottom, to form an individual product phase. The process rate is limited by the slowest stage, which is the deposit desorption. It is assumed that in the case of the resin in CO_3-form a closer deposit with higher adhesive properties is formed; therefore, more time is needed for it to flake away than in the case of using the anion exchanger in hydroxide form.

In order to increase the desorption rate and decrease the adsorbed metal amount the process was carried out at 60 °C. The effect of the increasing temperature produced a positive impact on the product yield (Table 1, Samples 2, 5). But the amount of the adsorbed deposit remained significant, 15 and 17 % for OH- and CO_3-forms, respectively. In the subsequent experiments, we used the temperature gradient: after the reaction proceeding for 1 h at 60 °C the mixture was

rapidly cooled to 15 °C in an ice bath. This procedure led to the rapid exfoliation of the surface deposit due to the difference in coefficients of thermal expansion of the surface deposit and resin. The indium content in the resin phase decreased to 2-3%, and the product yield increased up to 95 and 87 % (Table 1, samples 3, 6).

Table I: The influence of the reaction conditions on the yield of the product (deposition time - 1 h).

№	Product	Temperature, °C		Molar ratio fraction of surface deposit, %	Product yield, %
		Initial	Final		
1	In-OH	23	23	17	68
2		60	60	15	75
3		60	15	3	95
4	$In-CO_3$	23	23	27	62
5		60	60	17	70
6		60	15	2	87

The optimum reaction conditions providing up to 95 % yield of indium hydroxide were as follows: the strong base anion exchange resin in OH- or CO_3-form, with the concentration of $In_2(SO_4)_3$ solution being 0.25 M, processing time being 1 h at a temperature of 60 °C, followed by cooling to 15 °C in the ice bath.

Characterization of the products

The composition of the products obtained under the optimum reaction conditions using the anion resin in CO_3-form (named In-CO_3) and OH-form (named In-OH) was determined by elemental (atomic absorption spectroscopy, CHNS/O - analysis), and complex thermal analysis (Figure 2). Based on the obtained results, the elemental composition of as-precipitated products was established, which is represented by the following formulas: $In(OH)_{2.64}(CO_3)_{0.18}\cdot H_2O$ for the In-OH sample and $In(OH)_{1.94}(CO_3)_{0.53}\cdot H_2O$ for the In-CO_3 sample. The presence of impurity carbonate ions in the In-OH sample can be explained by the CO_2 adsorption from air by the anion resins in OH-form.[29] Also, hydroxide ions were detected in the In-CO_3 sample due to the hydrolysis of indium carbonate.

Figure 6 shows the diffraction patterns of the In-CO_3 and In-OH samples after their calcination at 400 °C. The diffraction peaks in both cases correspond to the cubic In_2O_3 (JCPDS file № 74-1990). No peaks evidencing other crystal phases were detected. The crystallite size, calculated using the Debye-Scherrer equation for the four most intensive peaks, was 15.8 nm for the In-OH sample and 14.3 nm for the In-CO_3 sample. According to the TEM data (Fig. 7), the particle size of the In-CO_3 sample was approximately 8-10 nm and for the In-OH sample was 10-12 nm, which is close to the XRD data. In addition, the specific surface area was measured using the BET model, being 73 and 62 m^2/g for In-CO_3 and In-OH, respectively. Based on these data, the particle size was calculated using the equation given in,[31] amounting to 13 and 11 nm, respectively. The obtained values of the particle size were in good agreement with the TEM data and with the calculated sizes from the XRD data.

Thus, the type of the resin counterions (OH or CO_3) had no significant effect on the particle size of the produced indium oxide. It is worth noting that the precursors, consisting of nanoscale particles, which were obtained by the anion resin exchange precipitation technique have high chemical activity and a large specific surface area.

Conclusion

In the present study, the process of anion resin exchange precipitation of indium (III) hydroxide by using the electrical conductivity measurement method, SEM, X-ray microanalysis and chemical analysis was thoroughly studied. Based on the obtained data, the mechanism of the process, proceeding through the stages of anion exchange between the anions of indium solution and the resin, precipitation of indium hydroxide on the surface of the resin beads and the rate-limiting stage of the surface deposit desorption with the formation of an individual product phase was proposed.

The optimum reaction conditions providing the maximum product yield were as follows: the strong base anion exchange resin in OH- or CO_3-form, with the concentration of $In_2(SO_4)_3$ solution being 0.25 M, processing time being 1 h at a temperature of 60 °C, followed by cooling to 15 °C in the ice bath. According to TG-DSC and elemental analysis, in the presence of the AV-17-8(OH) resin the product with the molecular formula $In(OH)_{2.64}(CO_3)_{0.18}\cdot H_2O$ was obtained, while in the case of AV-17-8(CO_3) the obtained product was $In(OH)_{1.94}(CO_3)_{0.53}\cdot H_2O$.

In addition, the as-prepared deposits after the heat treatment at 400 °C were transformed to impurity-free monophase In_2O_3 powders with the average particle size of 10-15 nm and specific surface area of 62-73 m^2g^{-1}. The obtained materials are promising as precursors for the preparation of indium tin oxide; they can also be used in modern electronics.

Materials and methods

Indium nitrate $In(NO_3)_3 \cdot 4.5H_2O$, indium chloride $InCl_3 \cdot 3H_2O$, indium sulfate $In_2(SO_4)_3 \cdot xH_2O$ were purchased from Sigma-Aldrich. The anion-exchange resin AV-17-8 was produced by "Azot" Corporation (Cherkassy, Ukraine) in the chloride form with grain size 0.25–0.5 mm (Russian GOST 20301-74). The conversion of resin to the hydroxyl or carbonate - form and the determination of its total exchange capacity, i.e., the total number of sites available for exchange, was carried out according to the techniques described in.[24,30] The total exchange capacity of the anion-exchange resin in the hydroxide form was 1.0 $meq \cdot g^{-1}$, and in the carbonate form - 0.7 $meq \cdot ml^{-1}$.

In typical experiments the calculated volume of AV-17-8(CO_3) or weight of AV-17-8(OH) taken in a 1,5 molar excess over the reaction (2 or 1, respectively) stoichiometry, was added to 0.25 M solution of indium salt. The mixture was stirred vigorously at a temperature of 20-60 ° C using a magnetic stirrer for a specified time: from 15 min to 24 h. To remove the anion exchange resin beads from the reaction products, a sieve with round holes 0.25 mm in diameter was

used, the precipitate was centrifuged, washed with distilled water and finally dried in air at 80 °C to form a precursor. The resin was also washed with distilled water, eluted three times with 1 M HNO_3 (10 ml portions) while stirring for 1 h. All the aqueous samples (eluates, stock solutions, dissolved precipitates) were analyzed for indium using a Perkin Elmer A Analyst 400 Atomic-Absorption Spectrometer (USA). The molar fraction of In^{3+} (χ, %) in each phase was calculated using the formula:

$$\chi = n^{eq} / n^{0} \cdot 100\%,$$

where n^{eq} is the number of moles In^{3+} in the phase (precipitate, anion exchange resin, stock solution), n^0 is the number of moles In^{3+} in the solution at the initial moment of time.

The specific electrical conductivity (SEC) of the reaction solutions was measured using a Multitest KSL-101 (Semiko company, Novosibirsk, Russia).

In_2O_3 samples were obtained by heat treatment of the precursors in a muffle furnace for 1 h at 400 °C.

The surface of the anion exchange resin beads during the precipitation was investigated by SEM microscopy. Small portions of resin (less than 1% of the total amount) were removed from the reaction vessel after a certain time interval (15 min, 30 min, 60 min, and 24 h), washed with distilled water, dried at 60 °C and fixed on an aluminum plate 5*7*0.3 mm using epoxy resin. Micrographs and elemental mapping of the resin beads surface were performed using a TM-3000

desktop scanning electron microscope (Hitachi, Japan) equipped with a BRUKER XFlash 430 H X-ray analyzer.

The thermochemical analysis of the precursors was conducted by thermogravimetry and differential scanning calorimetry (TG-DSC, NETZSCH STA449C) in the temperature range of 25–900 °C at a heating rate of 10 °C min^{-1} in flowing air (30 ml min^{-1}). The analysis of evolved gases during the sample heating was carried out using a quadrupole mass spectrometer QMS 403 C Aëolos (NETZSCH).

Powder X-ray diffraction was carried out using a Shimadzu XRD-7000S diffractometer equipped with a Cu Kα anode. The carbon content in the samples was determined using the Flash EA 1112 instrument from Thermo Fisher Scientific. Nitrogen adsorption was measured using an ASAP 2420 instrument (Micromeritics) at T = 77.3 K. The specific surface area was calculated using the BET model.

Transmission electron microscopy (TEM) was carried out using a HT-7700 instrument (Hitachi, Japan) operating at an accelerating voltage of 100 kV.

Acknowledgements

The work was supported by the Russian Foundation for Basic Research (RFBR): grant. No.18-33-00504. The authors thank the Federal Research Center "Krasnoyarsk Science Center of the Siberian Branch of the Russian Academy of Sciences" for using its facilities.

Figure captions

Fig.1. The time dependence of the specific electrical conductivity (SEC) of the reaction solutions during the anion resin exchange precipitation: (a) In-OH from 1 - $In_2(SO_4)_3$, 2 - $InCl_3$, 3 - In $(NO_3)_3$; (b) 1 - In-OH; 2 – In-CO_3 from $In_2(SO_4)_3$

Fig.2. TG, DSC and mass spectrum of the released gases during heating (H_2O, CO_2) for In-CO_3

Fig.3. Molar fraction of In^{3+} (χ) in the phases: 1 - precipitate, 2 - anion exchange resin, 3 - contact solution during the anion exchange precipitation In-OH (a) and In-CO_3 (b)

Fig.4. SEM micrographs of the grain surface of the anion resin AV-17-8 (CO_3) during the synthesis of In-CO_3

Fig.5. SEM micrograph of the surface deposit on the AV-17-8(CO_3) resin bead during the synthesis of In-CO_3, with the marked area for X-ray microanalysis (a) and mass fractions of the elements in this area (b)

Fig.6. The X-Ray Diffraction patterns of the In_2O_3 samples obtained for In-OH (1) and In-CO_3 (2)

Fig.7. The TEM micrographs and histograms of the particle size distribution of the In_2O_3, samples obtained for In-CO_3 (a) and In-OH (b)

References

(1) Lu, J. G., Chang, P. & Fan, Z. Quasi-one-dimensional metal oxide materials—Synthesis, properties and applications. *Mater. Sci. Eng. R Reports* **2006**, 52, 49–91.

(2) Exarhos, G. J. & Zhou, X.-D. Discovery-based design of transparent conducting oxide films. *Thin Solid Films* **2007**, 515, 7025–7052.

(3) Freeman A.J., Poeppelmeier K.R., Mason T.O., Chang R.P.H., M. T. J. Chemical and Thin-Film Strategies for New Transparent Conducting Oxides. *MRS Bull.* **2000**, 25, 45–51.

(4) Fedorov, P. I. & Akchurin, R. K. *Indii*. (Nauka, 2000).

(5) Granqvist, C. G. Transparent conductors as solar energy materials: A panoramic review. *Sol. Energy Mater. Sol. Cells* **2007**, 91, 1529–1598.

(6) Rembeza S., Voronov P., R. E. Synthesis and Physical Properties of Nanocomposites $(SnO_2)_x(In_2O_3)_{1-x}$ (x=0–1) for Gas Sensors and Optoelectronics. *Sensors Transducers J.* **2010**, 122, 46–54.

(7) Gilstrap, R. A., Capozzi, C. J., Carson, C. G., Gerhardt, R. A. & Summers, C. J. Synthesis of a Nonagglomerated Indium Tin Oxide Nanoparticle Dispersion. *Adv. Mater.* **2008**, 20, NA-NA.

(8) Li, C., Lian, S., Liu, Y., Liu, S. & Kang, Z. Preparation and photoluminescence study of mesoporous indium hydroxide nanorods. *Mater. Res. Bull.* **2010**, 45, 109–112.

(9) Lee, W. J. *et al.* Structural evolution of indium hydroxide powders prepared by a precipitation method. *J. Ceram. Process. Res.* **2018**, 19, 272–278.

(10) Frei, M. S. *et al.* Mechanism and microkinetics of methanol synthesis via CO2 hydrogenation on indium oxide. *J. Catal.* **2018**, 361, 313–321.

(11) Tao, X., Sun, L., Li, Z. & Zhao, Y. Side-by-Side $In(OH)_3$ and In_2O_3 Nanotubes: Synthesis and Optical Properties. *Nanoscale Res. Lett.* **2010**, 5, 383–388.

(12) Goh, K. W., Johan, M. R. & Wong, Y. H. Enhanced structural properties of In_2O_3 nanoparticles at lower calcination temperature synthesised by co-precipitation method. *Micro Nano Lett.* **2017**, 13, 270–275.

(13) Zhu, H., Wang, Y., Wang, N., Li, Y. & Yang, J. Hydrothermal synthesis of indium hydroxide nanocubes. *Mater. Lett.* **2004**, 58, 2631–2634.

(14) Zhuang, Z., Peng, Q., Liu, J., Wang, X. & Li, Y. Indium hydroxides, oxyhydroxides, and oxides nanocrystals series. *Inorg. Chem.* **2007**, 46, 5179–5187.

(15) Lin, L. T. *et al.* Monodisperse In_2O_3 nanoparticles synthesized by a novel solvothermal method with $In(OH)_3$ as precursors. *Mater. Res. Bull.* **2015**, 64, 139–145.

(16) Li, B. *et al.* In_2O_3 hollow microspheres: Synthesis from designed $In(OH)_3$ precursors and applications in gas sensors and photocatalysis. *Langmuir* **2006**, 22, 9380–9385.

(17) Du, J., Yang, M., Cha, S. N., Rhen, D. & Kang, M. Microcubes , and Nanorods : Synthesis and Optical Properties *Cryst. Growth Des.* **2008**, 8, 2312–2317.

(18) Yu, N., Dong, D., Qi, Y. & Gui, J. Growth of Indium Hydroxide Nanocubes

Film by Hydrothermal Method. *J. Nanosci. Nanotechnol.* **2017**, 17, 1476–1479.

(19) Ramanathan, G., Xavier, R. J. & Murali, K. R. Sol Gel Dip Coated Indium Oxide Films and Their Properties. *ECS Transactions* 2012, **41**, 33–38.

(20) Forsh, E. A. *et al.* Optical and photoelectrical properties of nanocrystalline indium oxide with small grains. *Thin Solid Films* **2015**, 595, 25–31.

(21) Gurlo, A. *et al.* Pressure-Induced Decomposition of Indium Hydroxide. *J. Am. Chem. Soc.* **2010**, 132, 12674–12678.

(22) Askarinejad, A., Iranpour, M., Bahramifar, N. & Morsali, A. Synthesis and characterisation of $In(OH)_3$ and In_2O_3 nanoparticles by sol-gel and solvothermal methods. *J. Exp. Nanosci.* **2010**, 5, 294–301.

(23) Pashkov, G. L. *et al.* Anion-Exchange Synthesis of Yttrium-Aluminum Garnet Powders. *Glas. Ceram. (English Transl. Steklo i Keramika)* **2016**, 73, 107–110.

(24) Ivantsov, R. *et al.* Synthesis and characterization of $Dy_3Fe_5O_{12}$ nanoparticles fabricated with the anion resin exchange precipitation method. *Mater. Sci. Eng. B Solid-State Mater. Adv. Technol.* **2017**, 226, 171–176.

(25) Taglieri G., Daniele V., M. L. Synthesizing Alkaline Earth Metal Hydroxides Nanoparticles through an Innovative, Single-Step and Eco-Friendly Method. *Solid State Phenom.* **2019**, 286, 3–14.

(26) Kobayashi, Y. *et al.* Fabrication of gadolinium hydroxide nanoparticles using ion-exchange resin and their MRI property. *J. Asian Ceram. Soc.* **2016**, 4, 138–142.

(27) Pashkov, G. L., Saikova, S. V. & Panteleeva, M. V. Reactive ion exchange processes of nonferrous metal leaching and dispersion material synthesis. *Theor. Found. Chem. Eng.* **2016**, 50, 575–581.

(28) Pashkov G.L., Sajkova S.V., Panteleeva M.V., Evsevskaya. N. P. *RF Patent* **2016**, No. 2 587 083, Byull. Izobret., No. 16.

(29) Pashkov, G. L., Saikova, S. V., Panteleeva, M. V. & Linok, E. V. Ion-exchange synthesis of α-modification of nickel hydroxide. *Theor. Found. Chem. Eng.* **2014**, 48, 671–676.

(30) Saikova, S. V., Panteleeva, M. V., Nikolaeva, R. B. & Pashkov, G. L. Optimal Conditions of Ion-Exchange Synthesis of Cobalt(II) Hydroxide with AV-17-8 Anion Exchanger in the OH Form. *Russ. J. Appl. Chem.* **2002**, 75, 1787–1790.

(31) Ayeshamariam A., Kashif M., Muthu Raja S., Sivaranjani S., Sanjeeviraja C., B. M. Synthesis and characterization of In_2O_3 nanoparticles. *J. Korean Phys. Soc.* **2014**, 64, 254–262.

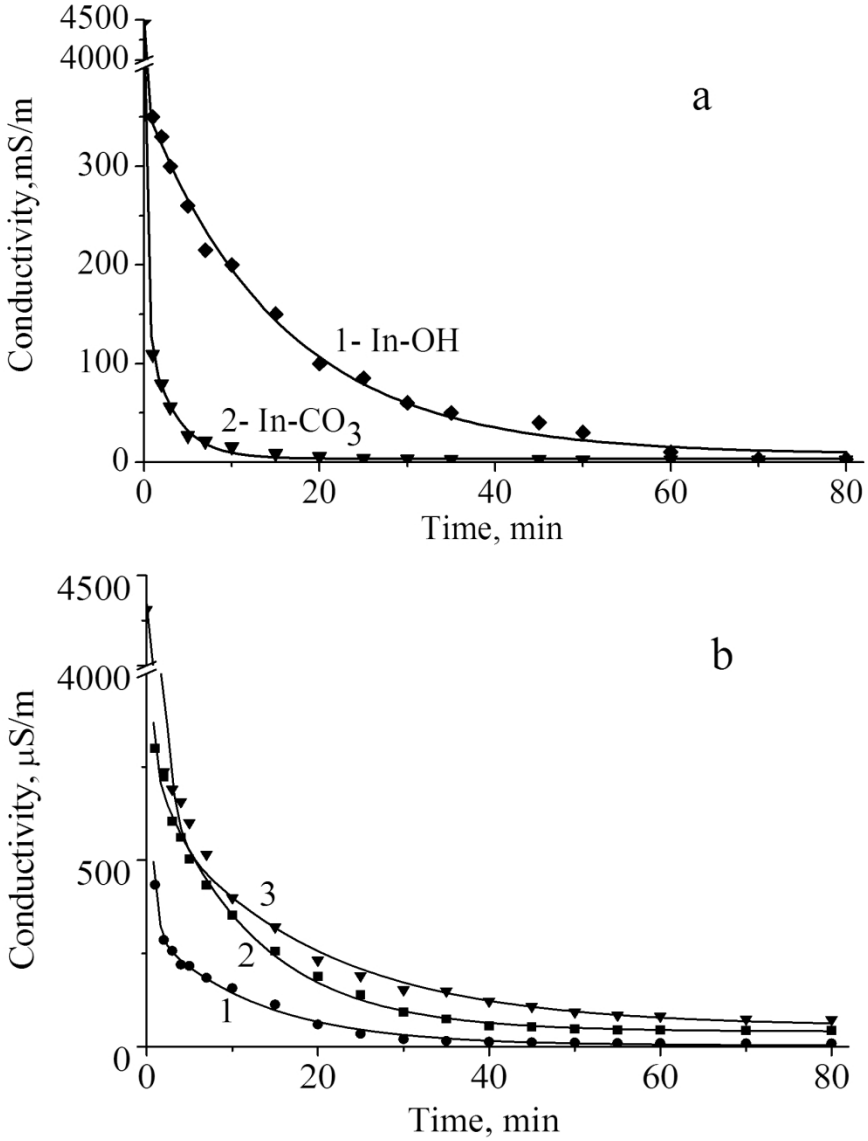

Fig.1. The time dependence of the specific electrical conductivity (SEC) of the reaction solutions during the anion resin exchange precipitation: (a) In-OH from 1 - In2(SO4)3, 2 - InCl3, 3 - In (NO3)3; (b) 1 - In-OH; 2 – In-CO3 from In2(SO4)3

156x199mm (300 x 300 DPI)

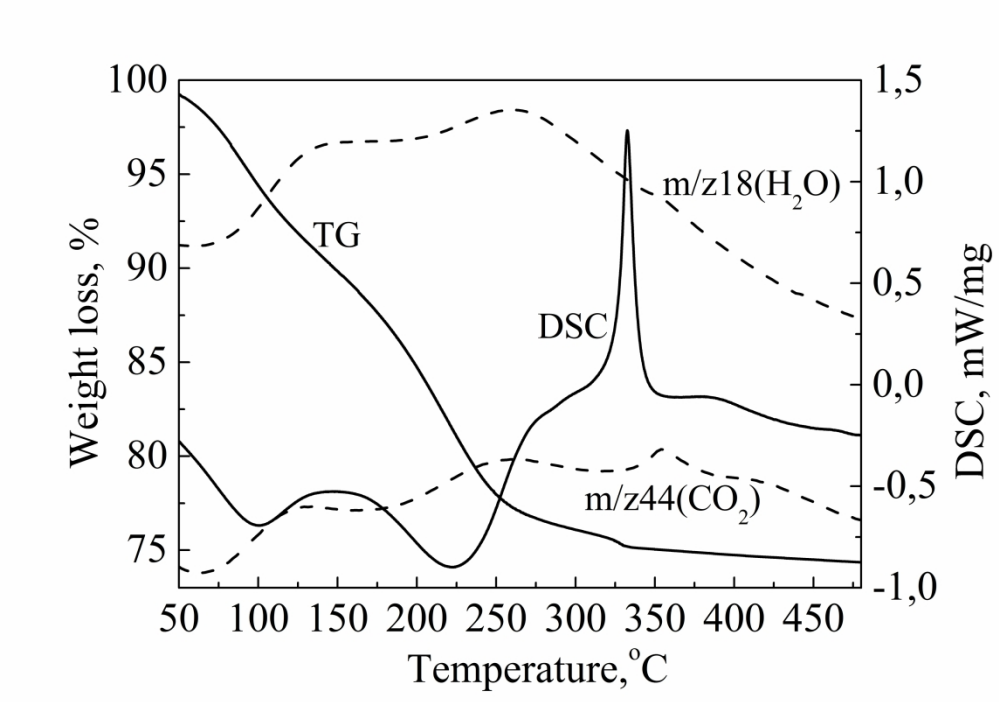

Fig.2. TG, DSC and mass spectrum of the released gases during heating (H2O, CO2) for In-CO3

152x107mm (600 x 600 DPI)

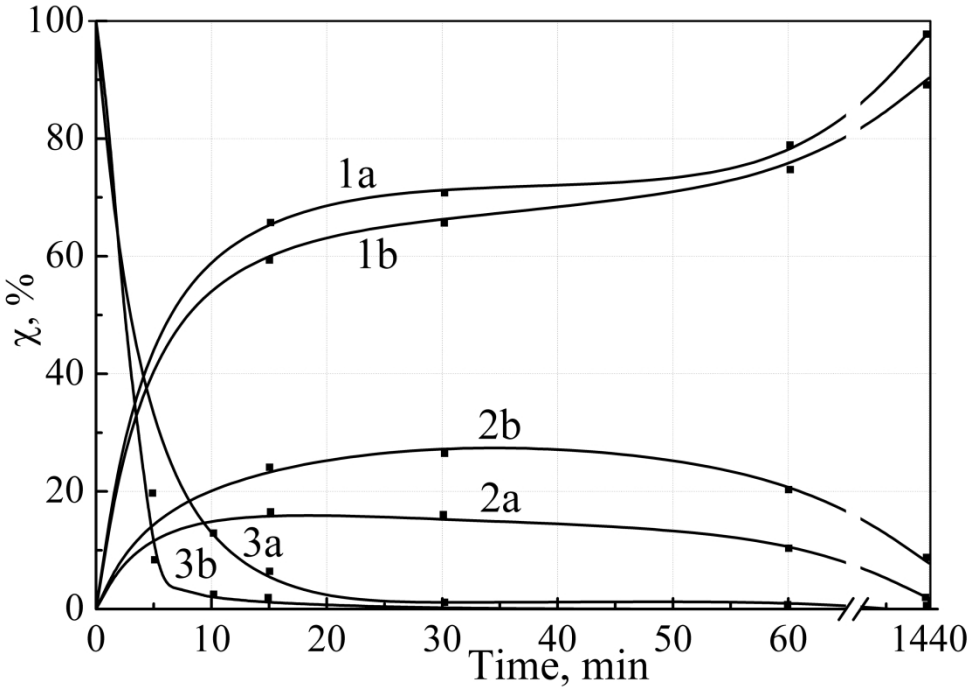

Fig.3. Molar fraction of In3+ (χ) in the phases: 1 - precipitate, 2 - anion exchange resin, 3 - contact solution during the anion exchange precipitation In-OH (a) and In-CO3 (b)

152x107mm (600 x 600 DPI)

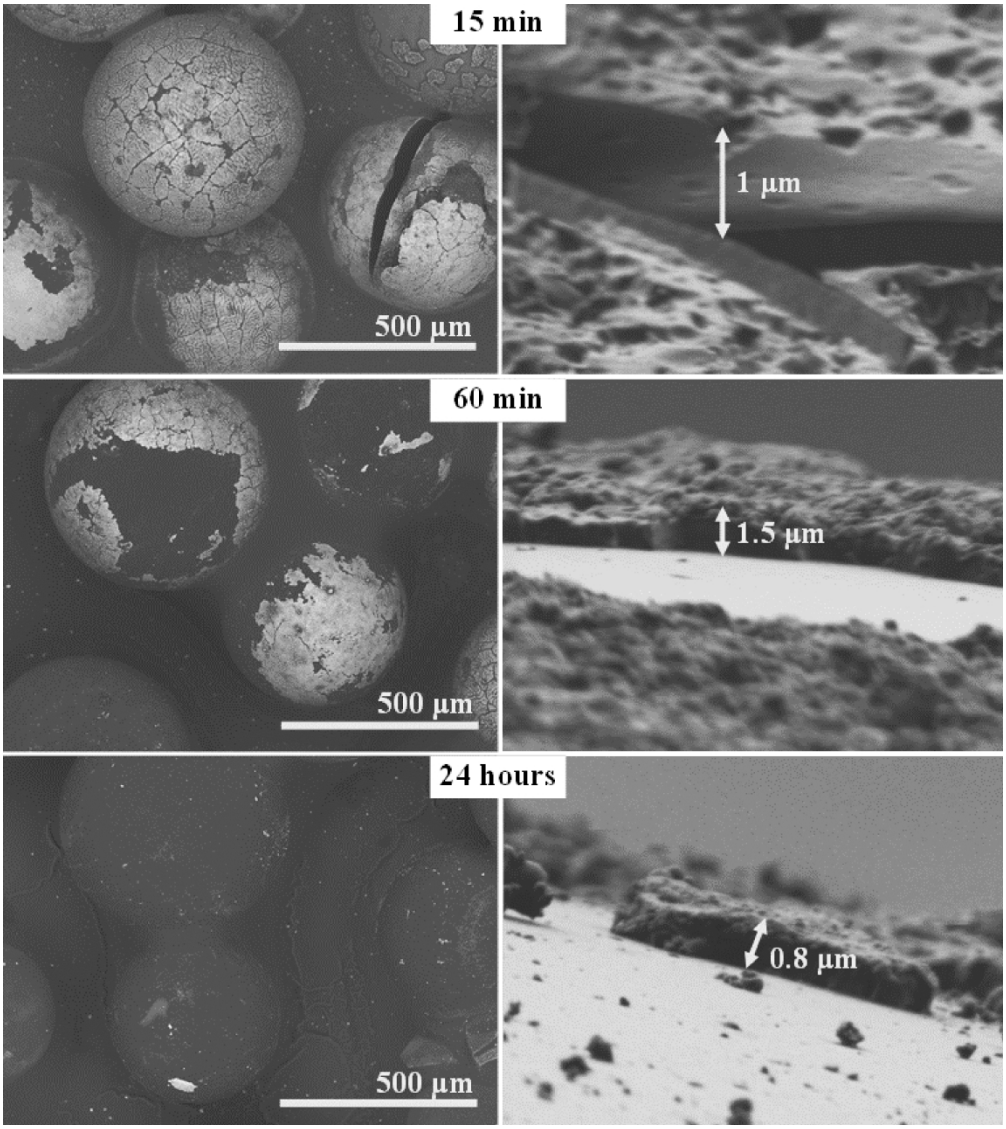

Fig.4. SEM micrographs of the grain surface of the anion resin AV-17-8 (CO3) during the synthesis of In-CO3

269x302mm (300 x 300 DPI)

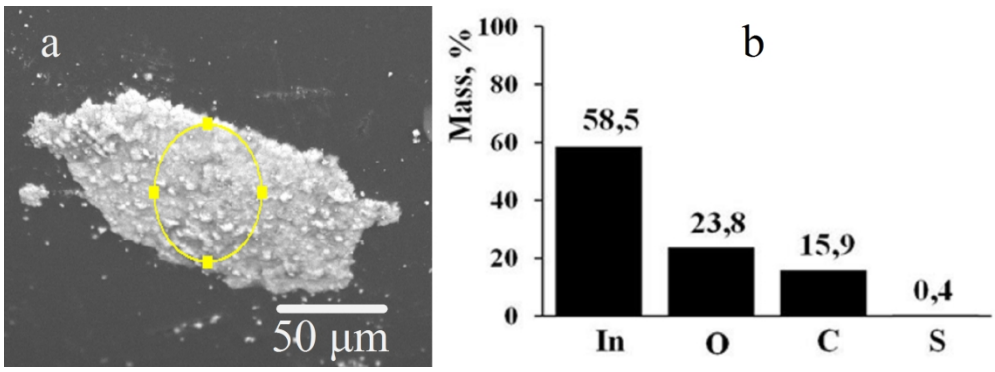

Fig.5. SEM micrograph of the surface deposit on the AV-17-8(CO3) resin bead during the synthesis of In-CO3, with the marked area for X-ray microanalysis (a) and mass fractions of the elements in this area (b)

184x66mm (300 x 300 DPI)

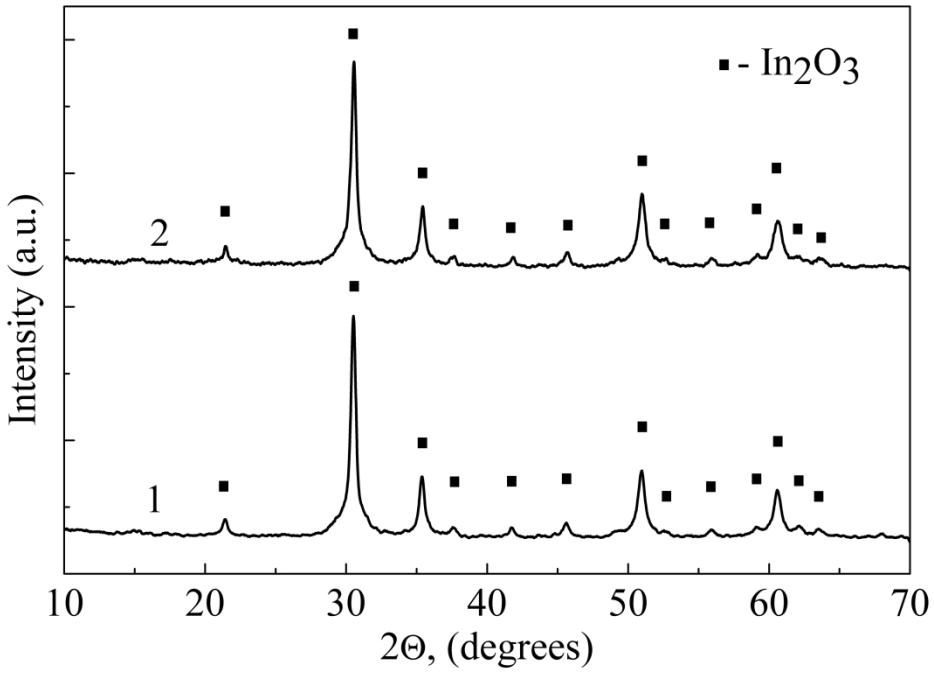

Fig.6. The X-Ray Diffraction patterns of the In2O3 samples obtained for In-OH (1) and In-CO3 (2)

152x107mm (600 x 600 DPI)

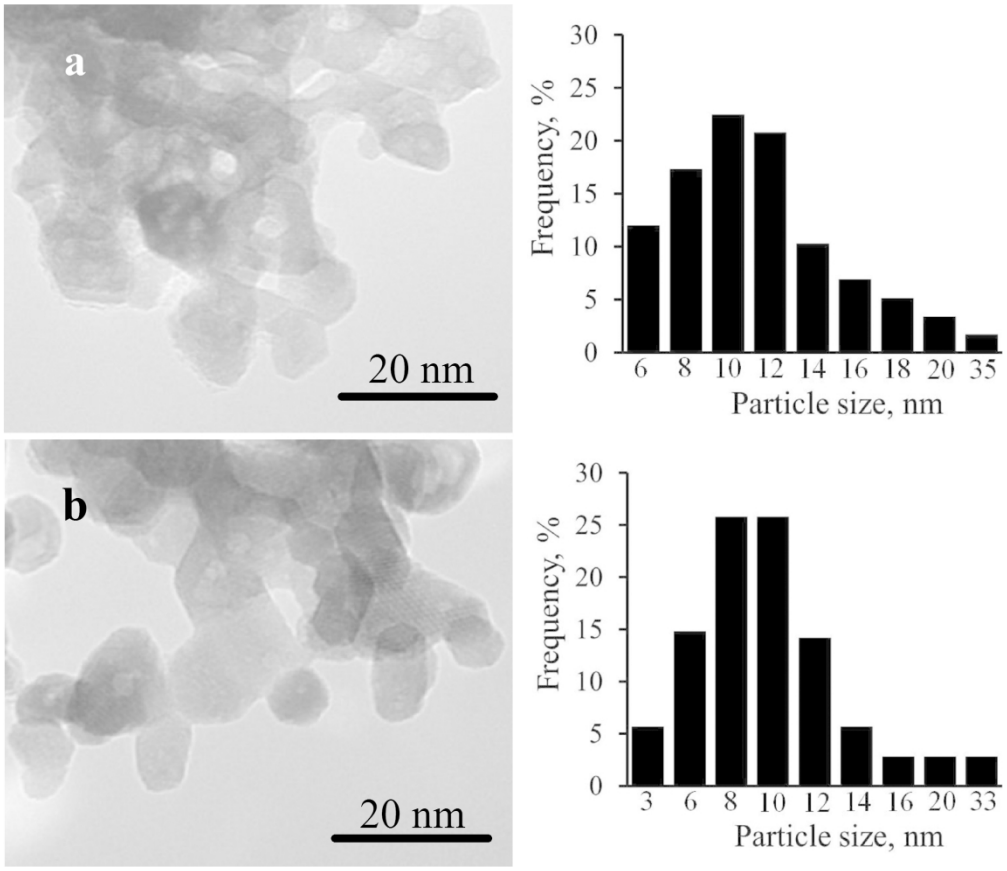

Fig.7. The TEM micrographs and histograms of the particle size distribution of the In2O3, samples obtained for In-CO3 (a) and In-OH (b)

202x174mm (300 x 300 DPI)